

1 **Role of ENSO conditions on particulate organic matter concentrations and elemental ratios**  
2 **in the Southern California Bight**

4 **Authors:** Adam J. Fagan<sup>1\*†</sup>, Allison R. Moreno<sup>2†</sup>, and Adam C. Martiny<sup>1,2,\*</sup>

6 **Affiliations:**

7 <sup>1</sup>Department of Earth System Science

8 <sup>2</sup>Department of Ecology and Evolutionary Biology

9 University of California

10 CA 92612, Irvine

12 <sup>†</sup>These authors contributed equally to this work

13 \*Corresponding Author

14 amartiny@uci.edu

16 **Keywords:**

17 MICRO, Ecological stoichiometry, Marine, ENSO, Redfield

19 **Running title:**

20 Linking ENSO with marine POM concentrations and ratios

22 **Abstract**

23 El Niño Southern Oscillation (ENSO) influences multi-year variation in sea-surface temperature  
24 and the intensity of upwelling in many Pacific regions. However, it is currently unknown how El  
25 Niño conditions will affect the concentration and elemental ratios of particulate organic matter  
26 (POM). To investigate this, we have been quantified POM weekly for six years (2012 to 2017) at  
27 the MICRO time-series station in the Southern California Bight. We found a strong influence of  
28 the 2015 El Niño on sea-surface temperature and phosphate concentration but to a lesser extent  
29 on nitrate availability. The 2015 El Niño also resulted in a short-term depression in POC and  
30 POP concentrations, whereas PON concentrations displayed an independent long-term decline  
31 regardless of the El Niño event. Reduced POM concentrations resulting from the 2015 El Niño  
32 occurred in parallel to high C:P and N:P ratios. Following the changes in PON, C:N continued to  
33 climb reaching ~9.4 at the end of our sampling. We suggest that an Eastern Pacific- vs. a Central  
34 Pacific-type El Niño as well as a switch in the Pacific Decadal Oscillation phase significantly  
35 altered the local response in POM concentrations and ratios.

36  
37 **Introduction**

38 El Niño Southern Oscillation (ENSO) is a recurring climate cycle leading to multi-year  
39 variation in ocean environmental conditions (Dijkstra and Burges, 2002; McPhaden, 2015). In  
40 the California Current System, ENSO regulates sea-surface temperature (SST), upwelling source  
41 and intensity, thermocline depth, and large-scale circulation patterns (Chavez, 2002; Checkley  
42 and Barth, 2009; McGowan et al., 1998). In the southern part of the California Current  
43 Ecosystem (i.e., the Southern California Bight, SCB), El Niño conditions are typically

44 manifested as periods of high temperature and low nutrient availability (Chavez, 2002; King and  
45 Barbeau, 2011; Tegner and Dayton, 1987). ENSO variability may have a negative effect on  
46 plankton growth and biomass accumulation, however this link has been elusive (Kim et al.,  
47 2009). Thus, it is currently unclear how coastal plankton will respond to recent ENSO-driven  
48 changes in ocean conditions.

49 There appears to be multiple modes of El Niño events including the Eastern-Pacific (EP)  
50 and Central-Pacific (CP) El Niño (Paek et al., 2017; Yu et al., 2012). The two types of El Niño  
51 conditions differentially regulate temperature anomalies including a shift in the regional location  
52 of maximum sea-surface temperature variability. A high positive temperature anomaly in the  
53 North Eastern Pacific Ocean is more indicative of an EP El Niño-type, whereas increased  
54 temperatures in the equatorial Pacific Ocean are typically associated with the CP El Niño-type  
55 (Paek et al., 2017). Furthermore, different El Niño modes result in spatially divergent patterns of  
56 declining vs. increasing phytoplankton biomass and growth (Racault et al., 2017). Generally a  
57 change in planktonic biomass and growth has an effect on the overall community structure. In  
58 the southern part of the California Current Ecosystem, the EP El Niño can result in significantly  
59 shift in community composition of phytoplankton. In contrast, CP El Niño has a proposed  
60 limited effect on phytoplankton in SCB. Thus, the mode of El Niño is predicted to differentially  
61 impact biogeochemical processes in SCB.

62 A core property of ocean biogeochemistry is the elemental composition and  
63 stoichiometric ratios of particulate organic matter (POM). C:N:P of marine communities have  
64 traditionally been considered static at Redfield proportions (106C:16N:1P; Redfield, 1958).  
65 However, phytoplankton acclimation and adaptation to different ocean environmental conditions  
66 can have a large impact on C:N:P (Moreno and Martiny, 2018). Temperature and nutrient  
67 limitation are currently thought to be the most important regulators of C:N:P in the surface ocean  
68 although the relative contribution of each factor is subject to much debate. Increasing  
69 temperature is predicted to correspond to higher C:P and N:P in phytoplankton due to a reduced  
70 allocation to P-rich ribosomes (Toseland et al., 2013). Nutrient limitation is predicted to lead to a  
71 reduced use of the respective nutrient and higher carbon-to-nutrient ratio although the effect may  
72 be higher for P vs. N limitation (Garcia et al., 2016). Temperature and nutrients may also affect  
73 stoichiometry via changes in phytoplankton community composition and growth physiology.  
74 Smaller cells thriving in warm, nutrient deplete waters are proposed to have higher C:N:P ratios  
75 compared to large cell types like diatoms (Klausmeier et al., 2004). Similarly, slower growing  
76 cells need fewer P-rich ribosomes and have higher C:N:P (Sterner and Elser, 2002). Thus, shifts  
77 in temperature and nutrient concentrations during El Niño conditions are expected to impact  
78 phytoplankton community composition, physiology, and associated C:N:P. Based on current  
79 theories for the regulation of phytoplankton elemental stoichiometry, we therefore predict higher  
80 temperature and nutrient depletion lead to elevated C:N:P.

81 Recent studies have demonstrated considerable regional and temporal variation in C:N:P  
82 (Martiny et al., 2013a, Moreno and Martiny, 2018). Higher C:N:P have been associated with  
83 warm, nutrient deplete ocean regions dominated by marine Cyanobacteria and other small  
84 plankton. In contrast, colder, nutrient replete regions with high abundance of larger  
85 phytoplankton like diatoms have depressed C:N:P. A parallel link between environmental  
86 changes and C:N:P was also observed in a past study in the Southern California Bight (Martiny

87 et al., 2016). Here, variation in POM concentrations and ratios corresponded to seasonal  
88 oscillations in environmental conditions and phytoplankton abundances. Specifically,  
89 winter/spring periods with low temperature, high nutrient concentrations and a dominance of  
90 large phytoplankton resulted in low C:N:P and vice-versa for warmer periods during the summer  
91 and fall. Similar links between environmental conditions, phytoplankton community structure  
92 and C:N:P were also found on weekly and multi-year time-scales (Martiny et al., 2016). Based  
93 on these observations, we predict that El Niño conditions will positively impact C:N:P, but the  
94 strength of the C:N:P response will be modulated by the mode of El Niño.

95 Here, we quantify the changes in SST, macronutrient concentrations, POM  
96 concentrations, and POM elemental stoichiometric ratios at the MICRO time-series in the  
97 Southern California Bight weekly from the beginning of 2012 to the end of 2017 covering the  
98 large El Niño event in 2015. Based on these observations, we aim to quantify how El Niño  
99 conditions influence ocean POM concentrations and stoichiometric ratios. We predict that  
100 annually temperature would be at the highest and macronutrients at the lowest due to an offshore  
101 damping in upwelling during the 2015 El Niño. Through the regulation of phytoplankton  
102 ecology, we should see low POM concentrations and high carbon-to-nutrient elemental ratios.  
103 The outcome of this study will allow us to further understand how climatic drivers of ocean  
104 environmental conditions affect the link between the C, N, and P biogeochemical cycles.

## 105 **Methods**

### 106 *Collection*

108 Surface water was collected weekly at the MICRO time-series (33.608°N and  
109 117.928°W; Martiny et al., 2016). Two autoclaved bottles are rinsed with ocean water and filled  
110 for processing in the lab. Water temperature data is collected from an automated shore station off  
111 of Newport Pier as part of the Southern California Coastal Ocean Observing Systems  
112 (SCCOOS).

113 Triplicate 300 ml samples for POC/PON or POP from each bottle are filtered within an  
114 hour of collection through pre-combusted (500°C, 5 h) 25 mm GF/F filters (Whatman, MA).  
115 Each filter is rinsed with Milli-Q water before being fitted in order to remove potential P  
116 residues. The filtrate from the initial filtration is collected and used for macronutrient  
117 quantification. The filtrate is filtered through a 0.2 µm syringe filter into a 50 ml tube. Triplicates  
118 are collected for both macronutrient and stored in the -20 °C freezer.

119

### 120 *Macronutrients*

121 Nitrate and phosphate samples were collected in prewashed 50 mL Falcon tubes and filtered  
122 through a 0.2 µm syringe filter and stored at -20°C until further analysis. Soluble reactive  
123 phosphorus (SRP) concentrations were determined using the magnesium induced co-  
124 precipitation (MAGIC) protocol and calculated against a potassium monobasic phosphate  
125 standard (Karl and Tien, 1992; Lomas et al., 2010). Nitrate samples were treated with a solution  
126 of ethylenediaminetetraacetate and passed through a column of copperized cadmium fillings  
127 (<http://bats.bios.edu/methods/chapter9.pdf>).

128

### 129 *Particulate Organic Carbon and Nitrogen*

130 After thawing, POC/PON filters were allowed to dry overnight at 65°C before being packed into  
131 a 30 mm tin capsule (CE Elantech, Lakewood, New Jersey). Samples were then analyzed for C  
132 and N content on a FlashEA 1112 nitrogen and carbon analyzer (Thermo Scientific, Waltham,  
133 Massachusetts), following the protocol of Sharp (1974). POC and PON concentrations were  
134 calibrated using known quantities of atropine.

135

### 136 *Particulate Organic Phosphorus*

137 POP filters are placed in combusted glass vials. Potassium Monobasic Phosphate (1.0  
138 mM-P) is used as a standard. 2 ml of Magnesium sulfate (0.017 M; Macron Fine Chemicals) are  
139 added to each vial, covered in tin foil, and put into an oven at 80 °C overnight. The vials are  
140 wrapped in tinfoil and placed into a 500 °C muffle oven for two hours. Once cooled to room  
141 temperature, 5 ml HCl (0.2 M; EMD) is added to each vial and then capped with a Teflon coated  
142 cap and placed into the 80 °C oven for 30 min and placed into a 15 ml glass centrifuge tube.  
143 Each vial is then washed with 5 ml Milli-Q water and then added to the tubes. 1 ml of mixed  
144 reagent is added to each of the tubes, centrifuged at 4000 rpm for one minute and stored in the  
145 dark for thirty minutes. Each standard and sample is quantified at 885 nm. This method is  
146 modified from Lomas et al., 2010.

147

### 148 *Data Analysis*

149 All analyses were done in Matlab (Mathworks, MA). Using the smooth function, a four  
150 point moving average was overlaid onto the raw data time-series plots. To determine potential  
151 covariations, a Pearson's correlation coefficient was calculated for each pair of variables,  
152 followed by a test of statistical significance ( $p$ -value  $\leq 0.05$ ). Sum of square analysis was  
153 conducted on linear regressions to quantify the monthly and annual contributions. To  
154 deseasonalize our time series parameters, we apply a seasonal adjustment using a stable seasonal  
155 filter applying a 53-point moving average, representing our weekly sampling.

156

### 157 *El Niño Impacts*

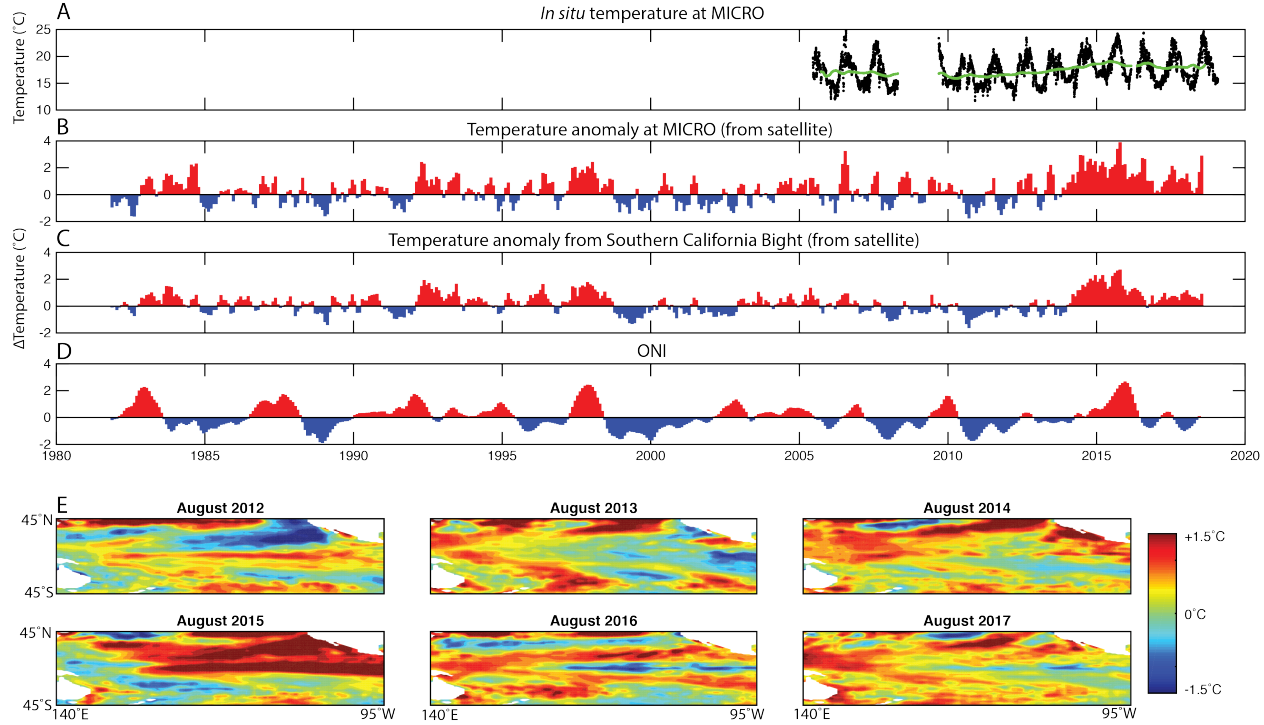
158 We used the ERSSTv5 estimate of the Oceanographic El Niño Index (ONI) (Huang et al.,  
159 2017). Regional temperature anomalies are derived by a linear interpolation of the weekly  
160 satellite SST optimum interpolation fields to daily fields then averaging the daily values over a  
161 month (Reynolds et al., 2002) from 1983 to 2018. To estimate the mean temperature anomaly for  
162 Southern California Bight region, we used satellite observations between 29° - 38°N and 115° -  
163 124°W.

164

## 165 **Results**

166 The Oceanic El Niño Index (ONI) data indicate that a strong El Niño event followed La  
167 Niña in 2015 (Figure 1). Generally, the ONI index data were significantly correlated with  
168 positive temperature anomalies at our MICRO site ( $R_{pearson} = 0.38, p < 1e-16$ ) and more broadly  
169 in the SCB ( $R_{pearson} = 0.44, p < 1e-22$ ). In support, El Niño periods including the 2015 event led  
170 to positive temperature anomalies of  $> 2^{\circ}\text{C}$ . One notable disconnect between ONI and the  
171 temperature anomalies at MICRO and in SCB was the period following the El Niño 2015 event.  
172 Here, ONI suggested a slightly negative anomaly and La Niña conditions. However, SCB and

173 our site still experienced strong positive temperature anomalies. This positive anomaly occurred  
 174 during both the summer and winter periods and might be related to an unusually high  
 175 temperature in the North Eastern Pacific Ocean (Di Lorenzo and Mantua, 2016). Thus, the 2015  
 176 El Niño event led to a positive temperature anomaly in SCB and MICRO, but the period  
 177 following was unexpectedly warm.

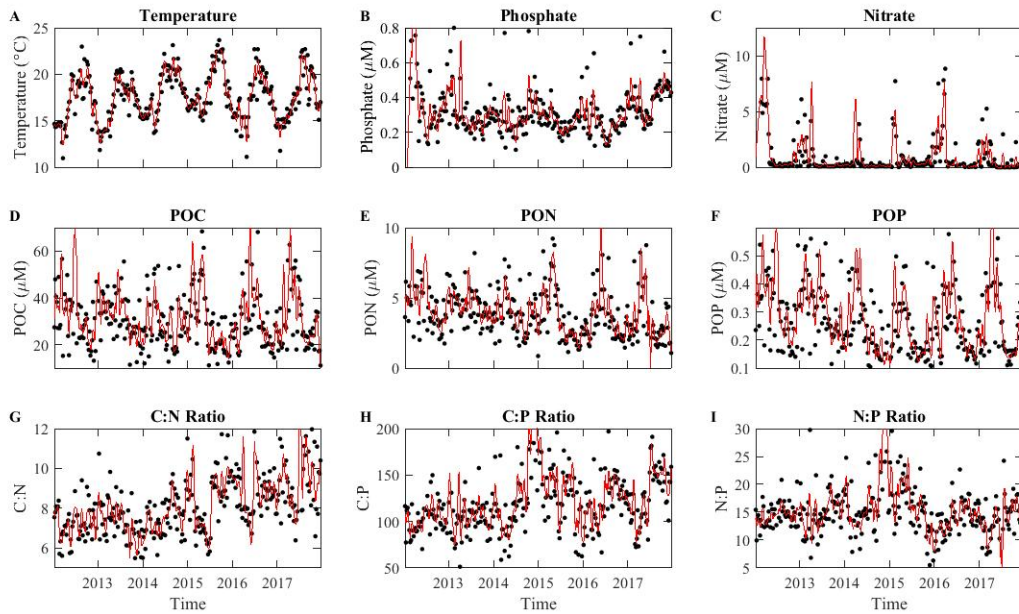


178 **Figure 1: Multi-year variation in temperature at MICRO and surrounding region.** A: The in  
 179 *180* situ daily temperature from 2005 to 2018 from the SCCOOS station on Newport Pier and the 2-  
 181 year moving average (green line). B: The temperature anomaly at the MICRO time-series  
 182 (estimated from satellite). C: The temperature anomaly in the Southern California Bight. D:  
 183 Oceanographic El Niño Index (ONI). E: Central Pacific Ocean temperature anomaly for August  
 184 throughout the time-series.

185 To understand the impact of El Niño conditions on the composition of marine POM, we  
 186 quantified weekly macronutrient concentrations, POM concentrations, and elemental  
 187 stoichiometric ratios from the beginning of 2012 to the end of 2017. Temperature oscillated  
 188 annually with a peak in August and trough in January (Figure 2A). In 2015, the average annual  
 189 temperature was higher than any other year at 22.4 °C, peaking to 23.7 °C (Figure 2A). As  
 190 described earlier, nutrient availability showed a strong seasonal anti-correlation with temperature  
 191 (Martiny et al., 2016) as well as some annual differences (Figure 2B). Nitrate concentrations also  
 192 oscillated in parallel with phosphate and reached extremely low or undetectable levels during the  
 193 summer (Figure 2C). In 2015, the nitrate level did not appear particularly low and stayed in  
 194 detectable ranges through most of the year. POM concentrations all peaked during the spring  
 195 bloom period and oscillated annually (Figure 2D-F). POC and POP concentrations did not show  
 196 any consistent long-term trends, whereas PON levels declined 26% throughout the time-series.  
 197 Although a slight increasing trend in C:N appeared from the start of the time series, a clear

199 increasing trend was obvious after 2014 (Figure 2G). Annually, C:P peaked during the  
 200 summer/fall at ~140 although we saw a big spike during the winter of 2014-2015 but this was  
 201 not an annually re-occurring phenomenon (Figure 2H). N:P followed the annual oscillation in  
 202 C:P with high values of 20 in the summer and also spiked during the same time periods (Figure  
 203 2I). Overall, we detected both seasonal and annual variation in both environmental conditions  
 204 and POM concentrations and ratios.

205



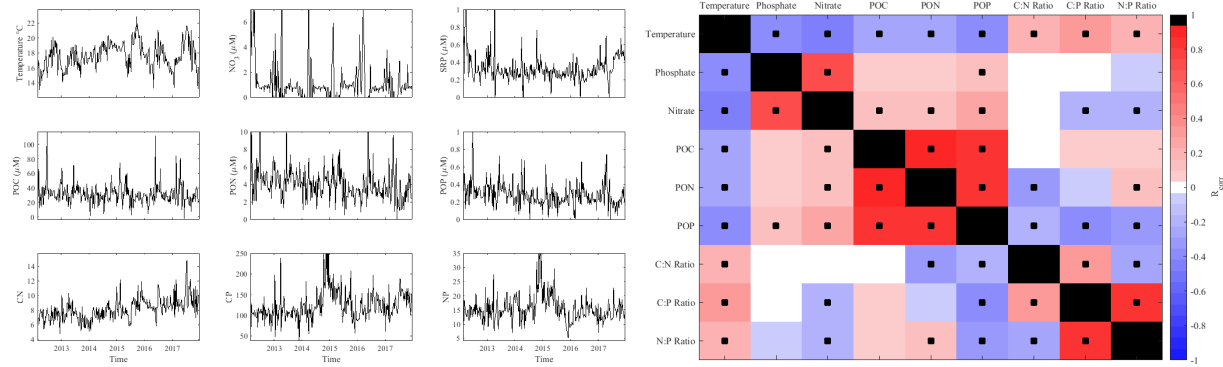
206

207 **Figure 2: Environmental conditions, macronutrient and POM concentrations and elemental**  
 208 **stoichiometric ratios over time at Newport Pier, Newport, CA.** The solid black points represent  
 209 the averaged data per week from the period of 1/1/2012 to 12/31/2017. The red line represents a  
 210 4-point moving average. Stoichiometric ratios are molar.

211

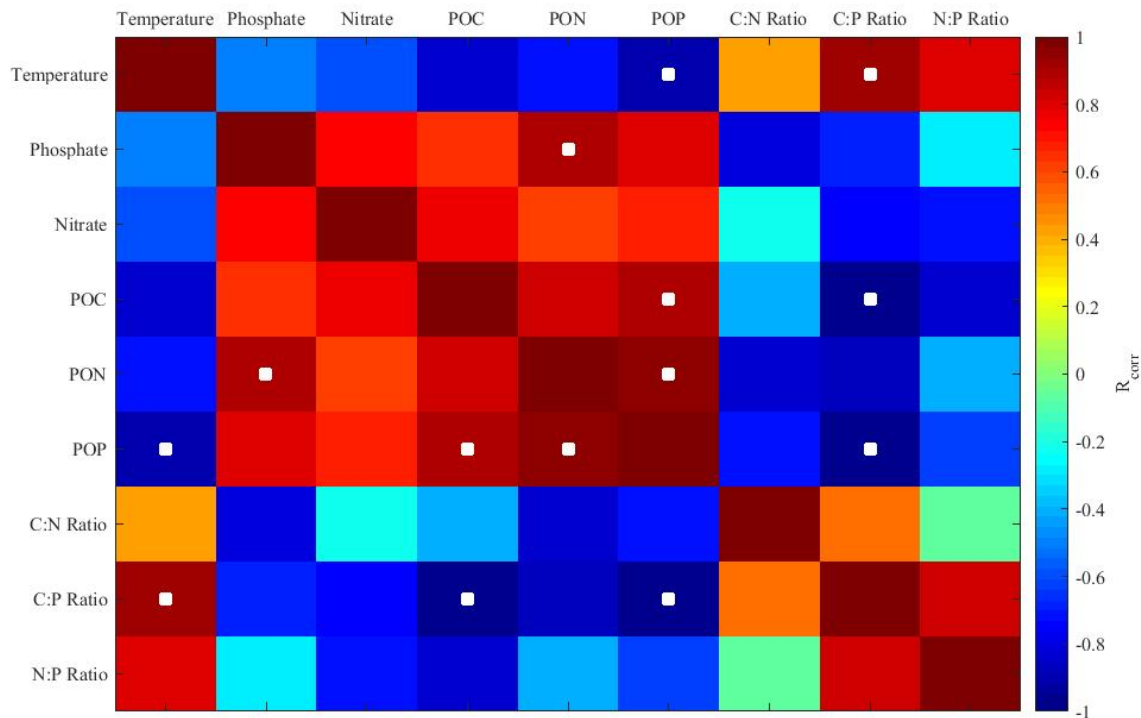
212 The MICRO study site experienced long-term shifts in oceanographic conditions (Figure  
 213 3). Seasonally detrended temperature concentrations has an increasing trend during the sampling  
 214 period (Figure 3A). Macronutrient and POM concentrations have a slight decreasing trend,  
 215 whereas the C:N and C:P ratios have increasing trends. The strongest positive correlations seen  
 216 in the seasonally detrended data is POC and PON with POP demonstrating that the POM  
 217 concentrations are linked (Figure 3B). Temperature is positively correlated with macronutrient  
 218 and POM concentration and negatively correlated with stoichiometric ratios (Figure 3B). Thus,  
 219 temperature is most likely the leading contributor to overall trends seen throughout the time  
 220 series.

221



222  
223 **Figure 3: Seasonally detrended values and correlations in environmental conditions,**  
224 **macronutrients and POM concentrations, and stoichiometric ratios.** A.) Deasonal trends  
225 over time for each factor. Statistical deseasonal trends quantified using a Mann-Kendal analysis  
226 ( $p < 0.05$ ). B.) Pearson correlation coefficient for each pair of factors. Redder squares signify a  
227 strong positive correlation between the two variables, while blue squares signify a strong  
228 negative correlation between the two variables. Large black squares represent a correlation of 1.  
229 The small black squares indicate that the correlation is statistically significant.

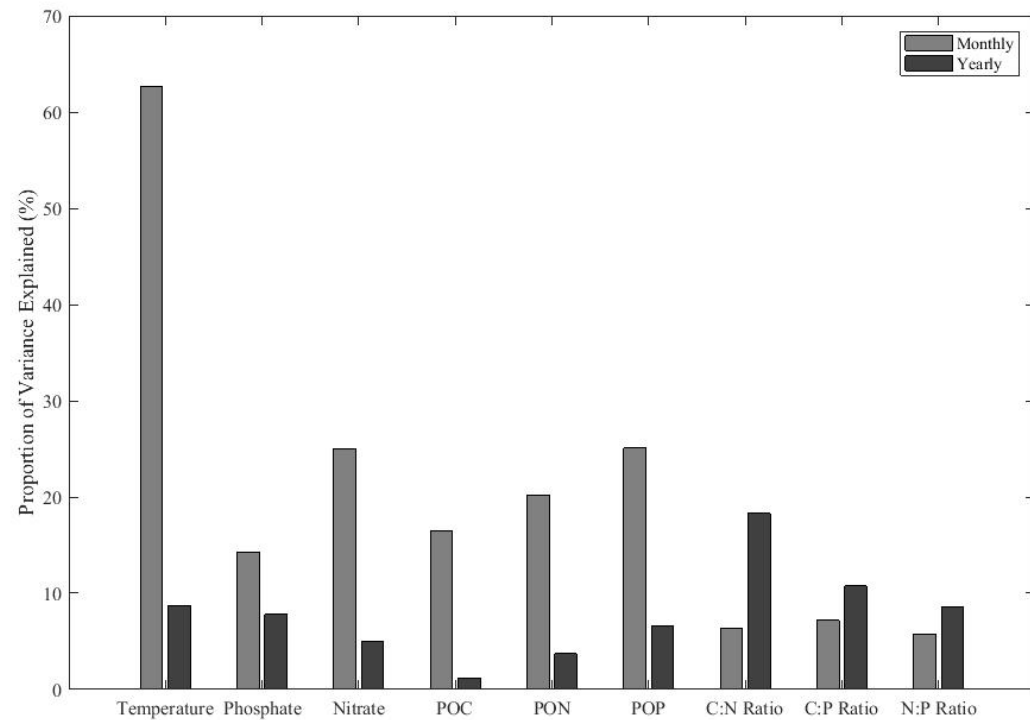
230  
231 Many factors showed significant positive or negative correlations (Figure 4).  
232 Temperature and nutrient concentrations show negative correlations, whereby warm periods had  
233 low nutrient concentrations and vice-versa for cold periods. POM concentrations were  
234 significantly correlated among each other and were generally correlated with environmental  
235 conditions. Warmer periods had low POM concentrations. In addition, C:P showed a positive  
236 relationship to temperature as we have higher C:P during the summer months. Thus, the  
237 observed correlations support earlier observations at MICRO as well as broader spatial patterns  
238 in the ocean (Martiny et al., 2013b, 2016).



239

240 **Figure 4: The Pearson correlation coefficient for each pair of factors.** Red squares signify a  
 241 strong positive correlation between the two variables, while blue squares signify a strong  
 242 negative correlation between the two variables. The white squares indicate that the correlation is  
 243 statistically significant.

244



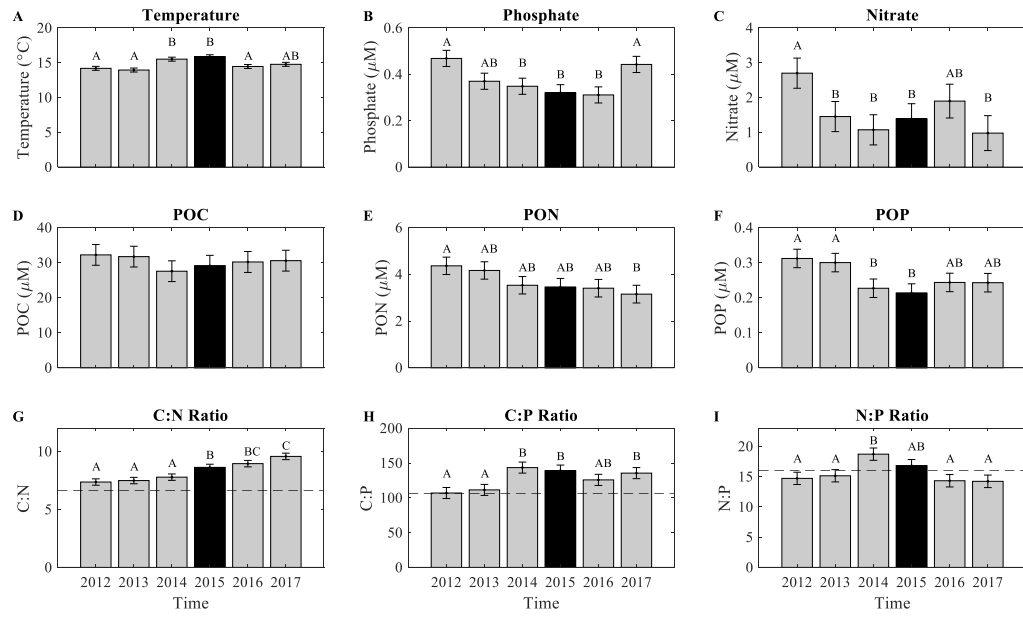
245

246 **Figure 5: The contribution of monthly and annual variation for environmental conditions and**  
247 **POM concentrations and ratios.** The remaining variance represents variance associated with  
248 short-term events and measurement errors. Proportions are calculated using the sum of squares  
249 from the linear regression data shown in Figure 6.

250  
251 We sought to quantify the amount of variability for environmental conditions, POM  
252 concentration, and ratio that is attributable to monthly versus annual variance. In general, we  
253 found that monthly compared to annual variance explained a higher proportion environmental  
254 metrics and POM concentrations (Figure 5). For temperature, monthly and annual variance  
255 explains a large fraction of total variability, with monthly changes making-up the majority.  
256 Monthly nitrate accounts for the second highest variability but the least in annual variability,  
257 with phosphate being vice versa. Similar to temperature and nutrients, monthly variability is  
258 greater among POM concentrations. As POM concentrations generally cycle in unison, there was  
259 less monthly variance in POM ratios. In contrast, we saw a larger proportion of variance in POM  
260 ratios between years. Monthly variation has more control on the environmental conditions and  
261 POM concentrations, whereas annual processes dominated for stoichiometric ratios. Thus, we  
262 should expect that especially POM stoichiometric ratio will be sensitive to El Niño events.  
263

#### 264 *Impact of the 2015 El Niño event*

265 The 2015 El Niño event had some impact on the POM concentrations and ratios at  
266 MICRO. Temperature was highest in 2015 (Figure 6A). The phosphate concentration was low in  
267 2015, although 2016 had lower levels (Figure 6B). However, nitrate concentrations were not  
268 particularly low that year and both 2014 and 2017 had lower levels (Figure 6C). POM  
269 concentrations showed divergent annual trends. Both POC and POP showed low levels in 2014  
270 and 2015, which could be indicative of an El Niño effect. In contrast, PON showed a declining  
271 trend throughout the sampling period leading to a 26% drop in concentration (Figure 6E). The  
272 change in PON coincided with a continually rising C:N and a high average ratio of 9.4 in 2017.  
273 (Figure 6G). In contrast, C:P and N:P were at their highest in late 2014 and all of 2015 (Fig. 2H  
274 and 2I). Thus, it appeared that the POM C:P and N:P were sensitive to the 2015 El Niño event,  
275 whereas C:N showed a divergent long-term increase.  
276



277

278 **Figure 6: The average annual variability in environmental conditions, POM concentrations,**  
 279 **and ratios.** The annual variations in August quantified using a linear decomposition of annual  
 280 and monthly variation. Error bars represent the standard deviation. The letters above each bar  
 281 represent a post hoc Tukey multiple comparison test ( $p < 0.05$ ), where similar letters show no  
 282 statistical difference. The dashed lines across the stoichiometric ratios indicates the static  
 283 Redfield ratio ( $C:N = 6.6$ ,  $C:P = 106$ , and  $N:P = 16$ ), strictly used for comparison purposes.

285 Discussion

Our time-series data suggests that the 2015 El Niño event impacted SST, phosphate conditions, POM concentrations, and stoichiometric ratios in our study region. The El Niño event resulted in unusually high temperature conditions and lower phosphate concentrations. Such environmental conditions are starting to resemble open-ocean conditions although the POM concentrations are still much higher than common oligotrophic regions. The high C:P and N:P ratios during the El Niño event support our hypothesis although the underlying drivers are unclear. Due to the strong seasonal link between temperature, phosphate and phytoplankton community at our site, we are unable to identify the exact mechanism resulting in high C:P and N:P.

295 The C:N ratio appeared to be regulated by different ecosystem processes than C:P and  
296 N:P. At our study site, we saw a long-term decline in PON concentration that led to high C:N.  
297 We hypothesize that the observed trend in C:N is regulated by a declining nitrate supply and N  
298 limitation (Moreno and Martiny, 2018, Geider and LaRoche, 2002). The nitrate concentration  
299 followed a different multi-year trajectory in comparison to phosphate and temperature leading to  
300 lower nitrate concentrations in later years. It is unclear if changing nitrate levels were driven by  
301 differences in nutrient run-off or by offshore shifts in source water and upwelling strength. In  
302 1998, the Santa Ana Regional Water Quality Control Board started regulating nitrogen run-off  
303 near our study site. This regulation has led to a decline in terrestrial nitrogen inputs (French et  
304 al., 2006). Furthermore, shifts in the source water for the SCB has led to declining  
305 phosphate:nitrate levels in subsurface waters (at the  $\sigma_\theta = 26.5$  kgm<sup>3</sup> isopycnal surface; Bograd

306 et al., 2014). Thus, there could be multiple ultimate causes for the observed declining nitrate  
307 level, but we predict that the lower nitrate availability and plankton N stress has proximately led  
308 to higher C:N ratios.

309 We expect that the observed correspondence between changing environmental conditions  
310 and C:N:P are in at least in part driven by shifts in phytoplankton community composition and  
311 physiological state. Our past work has demonstrated that increasing temperature and declining  
312 nutrient availability as observed during the El Niño event lead to increasing abundance of  
313 picophytoplankton lineages at the expense of larger eukaryotic phytoplankton (Martiny et al.,  
314 2016). Several studies have suggested that smaller phytoplankton lineages have higher C:P and  
315 N:P ratios (Klausmeier et al., 2004). Furthermore, phytoplankton will acclimate to increasing  
316 temperature and lower nutrient availability leading to higher cellular carbon-to-nutrient ratios.  
317 Both mechanisms could possibly explain the elevated C:P and N:P seen in late 2014 and 2015  
318 but our data does not allow for a direct identification of the underlying mechanism controlling  
319 the shift in POM stoichiometry.

320 El Niño events can vary in their expression leading to unique impacts on the  
321 environmental conditions and biogeochemical functioning of the SCB (Capotondi et al., 2015;  
322 Jacox et al., 2016). The 2015 event is likely an ‘Eastern Pacific’ type leading to a temperature  
323 anomaly in the North Eastern Pacific Ocean (Paek et al., 2017). However, there was also a strong  
324 temperature anomaly in the equatorial section of the Pacific and a high overall warming of most  
325 of the eastern part of the basin. As such, the biogeochemical impact of the 2015 El Niño event  
326 may diverge from a traditional ‘Central Pacific’ event. In addition to the El Niño event, we also  
327 saw a strong positive temperature and negative nitrate anomaly in 2016 and 2017. Such a long  
328 term warming of the region may be caused by a shift in the Pacific Decadal Oscillation (PDO;  
329 Newman et al., 2016). A positive PDO leads to overall high temperatures in the central/eastern  
330 part of the Pacific Ocean (Mantua et al., 1997) and a  $>2^{\circ}\text{C}$  temperature anomaly in the SCB. The  
331 underlying physical driver of the PDO is currently not clear but a shift in the phase could suggest  
332 elevated temperatures in the SCB for years to come. This would further lead to low POM  
333 concentrations but high C:nutrient ratios.

334 El Niño events can act as a natural ‘experiment’ to understand climate change effects on  
335 POM concentrations and stoichiometric ratios. Future climate scenarios predict increased SST  
336 and more stratified waters and El Niño events share these characteristics. Due to the offshore  
337 topography at MICRO, the local conditions share similarities with pelagic waters rather than  
338 typical coastal regions. Thus, our findings suggest that elevated temperature cause changes in  
339 nutrient availability phytoplankton ecology with clear implications for POM concentrations and  
340 ratios. However, it is unclear whether or not future El Niño events will superimpose on or blend  
341 into the already high ocean temperatures in the region. If the former, we predict large changes in  
342 the biogeochemical and ecosystem functioning of the SCB in the future.

343  
344

### 345 **Acknowledgement**

346 We would like to thank Professor Yu for advice on ENSO cycles, and Tanya Lam, Sarah Bowen,  
347 and Jenna Lee for contributing to the MICRO time-series. Financial support for this work was  
348 provided by the UCI Undergraduate Research Opportunities Program (to AF), NSF Graduate  
349 Research Fellowship Program (to ARM) and NSF Biological Oceanography (OCE-1848576 to  
350 ACM).

351 **References**

352 Bograd, S. J., Pozo, M., Di, E., Castro, C. G., Schroeder, I. D., Goericke, R., et al. (2014). Changes in  
 353 source waters to the Southern California Bight. *Deep. Res. Part II*, 1–11.  
 354 doi:10.1016/j.dsr2.2014.04.009.

355 Capotondi, A., Wittenberg, A. T., Newman, M., Di Lorenzo, E., Yu, J. Y., Braconnot, P., et al. (2015).  
 356 Understanding enso diversity. *Bull. Am. Meteorol. Soc.* 96, 921–938. doi:10.1175/BAMS-D-13-  
 357 00117.1.

358 Chavez, F. P. (2002). Biological and chemical consequences of the 1997-1998 El Niño in central  
 359 California waters Biological and chemical consequences of the 1997 – 1998 El Niño in central  
 360 California waters. *Prog. Oceanogr.* 54, 205–232.

361 Checkley, D. M., and Barth, J. A. (2009). Progress in Oceanography Patterns and processes in the  
 362 California Current System. *Prog. Oceanogr.* 83, 49–64. doi:10.1016/j.pocean.2009.07.028.

363 Di Lorenzo, E., and Mantua, N. (2016). Multi-year persistence of the 2014/15 North Pacific marine  
 364 heatwave. *Nat. Clim. Chang.* 6, 1042–1047. doi:10.1038/nclimate3082.

365 Dijkstra, H. A., and Burges, G. (2002). Fluid Dynamics of El Niño Variability. *Annu. Rev. Fluid Mech.*,  
 366 531–558. doi:10.1146/annurev.physchem.57.032905.104621.

367 French, C., Wu, L., Meixner, T., Kabashima, J., and Jury, W. A. (2006). Modeling nitrogen transport in  
 368 the Newport Bay / San Diego Creek watershed of Southern California. *Agric. Water Manag.* 81,  
 369 199–215. doi:10.1016/j.agwat.2005.03.006.

370 Huang, B., Thorne, P. W., Banzon, V. F., Boyer, T., Chepurin, G., Lawrimore, J. H., et al. (2017).  
 371 Extended Reconstructed Sea Surface Temperature , Version 5 (ERSSTv5): Upgrades , Validations  
 372 , and Intercomparisons. *Am. Meterological Soc.* 5, 8179–8205. doi:10.1175/JCLI-D-16-0836.1.

373 Jacox, M. G., Hazen, E. L., Zaba, K. D., Rudnick, D. L., Edwards, C. A., Moore, A. M., et al. (2016).  
 374 Impacts of the 2015–2016 El Niño on the California Current System: Early assessment and  
 375 comparison to past events. *Geophys. Res. Lett.* 43, 7072–7080. doi:10.1002/2016GL069716.

376 Karl, D. M., and Tien, G. (1992). MAGIC: A sensitive and precise method for measuring dissolved  
 377 phosphorus in aquatic environments. *Limnol. Oceanogr.* 37, 105–116.  
 378 doi:10.4319/lo.1992.37.1.0105.

379 Kim, H., Webster, P. J., and Curry, J. A. (2009). Impact of Shifting Patterns of Pacific Ocean Warming  
 380 on North Atlantic Tropical Cyclones. *Science (80-)*. 325, 77–80.

381 King, A. L., and Barbeau, K. A. (2011). Dissolved iron and macronutrient distributions in the southern  
 382 California Current System. *J. Geophys. Res. Ocean.* 116. doi:10.1029/2010JC006324.

383 Lomas, M. W., Burke, A. L., Lomas, D. A., Bell, D. W., Shen, C., Dyhrman, S. T., et al. (2010). Sargasso  
 384 Sea phosphorus biogeochemistry: an important role for dissolved organic phosphorus (DOP).  
 385 *Biogeosciences* 7, 695–710. doi:10.5194/bg-7-695-2010.

386 Mantua, N. J., Hare, S. R., Zhang, Y., Wallace, J. M., and Francis, R. C. (1997). A Pacific Interdecadal  
 387 Climate Oscillation with Impacts on Salmon Production. *Bull. Am. Meteorol. Soc.*, 1069–1079.

388 Martiny, A. C., Pham, C. T. A., Primeau, F. W., Vrugt, J. A., Moore, J. K., Levin, S. A., et al. (2013a).  
 389 Strong latitudinal patterns in the elemental ratios of marine plankton and organic matter. *Nat.*  
 390 *Geosci.* 6, 1–5. doi:10.1038/ngeo1757.

391 Martiny, A. C., Talarmin, A., Mouginot, C., Lee, J. A., Huang, J. S., Gellene, A. G., et al. (2016).  
 392 Biogeochemical interactions control a temporal succession in the elemental composition of marine  
 393 communities. *Limnol. Oceanogr.* 61, 531–542. doi:10.1002/lno.10233.

394 Martiny, A. C., Vrugt, J. A., Primeau, F. W., and Lomas, M. W. (2013b). Regional variation in the  
 395 particulate organic carbon to nitrogen ratio in the surface ocean. *Global Biogeochem. Cycles* 27,  
 396 723–731. doi:10.1002/gbc.20061.

397 McGowan, J. A., Cayan, D. R., and Dorman, L. M. (1998). Climate-Ocean Variability and Ecosystem  
 398 Response in the Northeast Pacific. *Science (80-)*. 281.

399 McPhaden, M. J. (2015). Playing hide and seek with El Niño. *Nat. Clim. Chang.* 5, 791–795.  
 400 doi:10.1038/nclimate2775.

401 Moreno, A. R., and Martiny, A. C. (2018). Ecological Stoichiometry of Ocean Plankton. *Ann. Rev. Mar.*

402 *Sci.* 10, 43–69. doi:10.1146/annurev-marine-121916-063126.

403 Newman, M., Alexander, M. A., Ault, T. R., Cobb, K. M., Deser, C., Di Lorenzo, E., et al. (2016). The  
404 Pacific Decadal Oscillation, Revisited. *Am. Meterological Soc.* 29, 4399–4427. doi:10.1175/JCLI-  
405 D-15-0508.1.

406 Paek, H., Yu, J. Y., and Qian, C. (2017). Why were the 2015/2016 and 1997/1998 extreme El Niños  
407 different? *Geophys. Res. Lett.* 44, 1848–1856. doi:10.1002/2016GL071515.

408 Racault, M.-F., Sathyendranath, S., Brewin, R. J. W., Raitsos, D. E., Jackson, T., and Platt, T. (2017).  
409 Impact of El Niño Variability on Oceanic Phytoplankton. *Front. Mar. Sci.* 4, 1–15.  
410 doi:10.3389/fmars.2017.00133.

411 Redfield, A. C. (1958). The biological control of the chemical factors in the environment. *Am. Sci.* 46, 1–  
412 18.

413 Reynolds, R. W., Rayner, N. A., Smith, T. M., Stoker, D. C., and Wang, W. (2002). An Improved In Situ  
414 and Satellite SST Analysis for Climate. *J. Clim.* 15, 1609–1625.

415 Sharp, J. H. (1974). Improved analysis for “particulate” organic carbon and nitrogen from seawater.  
416 *Limnol. Oceanogr.* 19, 984–989. doi:10.4319/lo.1974.19.6.0984.

417 Tegner, M. J., and Dayton, P. K. (1987). El Nino Effects on Southern California Kelp Forest  
418 Communities. *Adv. Ecol. Res.* 17, 243–279.

419 Toseland, A., Daines, S. J., Clark, J. R., Kirkham, A., Strauss, J., Uhlig, C., et al. (2013). The impact of  
420 temperature on marine phytoplankton resource allocation and metabolism. *Nat. Clim. Chang.* 3,  
421 979–984. doi:10.1038/nclimate1989.

422 Yu, J. Y., Zou, Y., Kim, S. T., and Lee, T. (2012). The changing impact of El Nio on US winter  
423 temperatures. *Geophys. Res. Lett.* 39. doi:10.1029/2012GL052483.

424